High-speed X-ray images of triggered lightning dart leaders

J. R. Dwyer,[1] M. Schaal,[1] H. K. Rassoul,[1] M. A. Uman,[2] D. M. Jordan,[2] and D. Hill[2]

Received 18 March 2011; revised 7 June 2011; accepted 3 August 2011; published 26 October 2011.

[1] We present the first high-time resolution two-dimensional images of X-ray emissions from lightning. The images were recorded at a rate of 10 million per second using a new pinhole-type camera, located 44 m from rocket-and-wire-triggered lightning. We report observations of two dart leaders, one in each of two lightning flashes triggered during the summer of 2010 in north-central Florida. In both events, as the dart leader approached the ground, the X-ray source was also seen to descend along the previous lightning channel. For the second event, the X-ray source exhibited a downward speed of 4.5×10^7 m/s, in agreement with independent *dE/dt* time-of-arrival (TOA) measurements of the speed of the dart leader front, demonstrating that the dart leader front was the source of the X-ray emission. The camera also recorded bursts of MeV gamma rays originating from the dart leader and/or the ground attachment process of the leader. Overall, these results provide new insight into the production of energetic radiation and the propagation and attachment of lightning, all of which remain poorly understood.

Citation: Dwyer, J. R., M. Schaal, H. K. Rassoul, M. A. Uman, D. M. Jordan, and D. Hill (2011), High-speed X-ray images of triggered lightning dart leaders, *J. Geophys. Res.*, *116*, D20208, doi:10.1029/2011JD015973.

1. Introduction

[2] Lightning is the only natural phenomenon on Earth that strongly emits electromagnetic fields over the wide frequency range from a few hertz (e.g., *Q* bursts) to 10^{21} Hz (gamma radiation). Because a given phenomenon often appears quite different in different frequency ranges, with different processes and structures being illuminated, it is desirable to examine the previously unstudied images of lightning in X-radiation. In this paper, we present the first X-ray images of lightning.

[3] That X-rays could be produced by runaway electrons in thunderstorm electric fields was first postulated by C. T. R. Wilson [*Wilson*, 1925], and X-rays associated with thunderstorm fields have been observed [*Shaw*, 1967; *Parks et al.*, 1981; *McCarthy and Parks*, 1985; *Eack et al.*, 1996a, 1996b; *Tsuchiya et al.*, 2007]. However, these X-ray emissions appear to be associated with the large-scale electric fields associated with the thunderclouds and not with lightning processes. It was only recently established that lightning also emits X-rays [*Moore et al.*, 2001; *Dwyer et al.*, 2003]. In a series of experiments beginning in 2002 at the University of Florida/Florida Tech International Center for Lightning Research and Testing (ICLRT) at Camp Blanding, Florida, it was found that lightning produces significant X-ray emissions in the 100 keV range during the stepped leader phase of natural lightning and during the dart leader phase of natural and rocket-and-wire-triggered lightning, with the most intense emissions detected immediately before the return stroke during the attachment process [*Dwyer et al.*, 2004, 2005a; *Howard et al.*, 2008; *Saleh et al.*, 2009; *Howard et al.*, 2010]. Since the triggering wire completely vaporizes before the recorded leader-return stroke sequence in triggered lightning occurs and since the density of the vaporized copper atoms is likely small compared with that of the surrounding air, bremsstrahlung emissions from energetic electrons interacting with air atoms are expected to dominate the X-ray emissions. In addition, the recorded X-ray energies are all greater than 30 keV, so X-ray fluorescent lines are not important. As a result, the wire used in rocket-triggered lightning should not affect the X-ray observations. The similarity of the X-ray emissions between triggered and natural lightning and the similarity between the early and later return strokes for triggered lightning support this hypothesis.

[4] Even though progress has been made in quantifying some properties of the lightning-leader X-ray emission, the mechanisms for producing the X-rays and the nature of the source regions have remained uncertain. It is thought that the X-rays are produced by bremsstrahlung emissions from energetic runaway electrons accelerated by very strong electric fields (>30 MV/m), at least 10 times the electrical breakdown field in air [*Dwyer*, 2004; *Gurevich*, 1961; *Moss et al.*, 2006]. However, exactly how and where lightning produces these strong fields are still unclear. We note that, based on the measured energy spectra and fluence of the X-rays, the relativistic runaway electron avalanche (RREA) mechanism [*Gurevich et al.*, 1992], which requires smaller electric field magnitudes, does not appear to be responsible for the runaway electron production and the X-ray emission associated with lightning [*Dwyer*, 2004]. Furthermore, despite decades of research, the physics of lightning propa-

[1]Department of Physics and Space Sciences, Florida Institute of Technology, Melbourne, Florida, USA.
[2]Department of Electrical and Computer Engineering, University of Florida, Gainesville, Florida, USA.

0148-0227/11/2011JD015973

Figure 1. Photograph of the X-ray camera in front of the rocket-launch tower used to trigger lightning at the ICLRT (courtesy of D. Hill).

gation and attachment remain poorly understood [*Rakov and Uman*, 2003]. In an attempt to ameliorate this situation, we have constructed a new X-ray imaging camera and operated it at the ICLRT in order to produce two-dimensional (2-D) "photos" and "movies" of the X-ray source regions of lightning. Such images not only provide new information about how energetic electrons are accelerated by lightning, but they provide a novel view of lightning, potentially identifying the dynamics of the high electric field regions and related charge sources, observations that are difficult to make with other methods.

2. Instrumentation

[5] Imaging lightning in X-rays presents several unique challenges that preclude the use of standard X-ray imaging technologies: (1) The X-ray emissions arrive in very short, but intense, bursts on submicrosecond time scales, requiring fast detectors with fast electronics; (2) the emission is very energetic, with photon energies ranging from tens of keV to several MeV. One of the few practical methods for imaging such X-rays is using a mask with a restricted aperture such as a pinhole-type camera. However, in order to block the X-rays, the mask must be massive; and (3) the X-ray emission that is detectable from ground-based instruments originates from an extended vertical channel structure hundreds of meters long, requiring the camera with a wide field of view to be placed a considerable distance (e.g., >40 m) from the lightning channel. However, the camera cannot be placed too far from the channel, since X-rays typically only propagate a few hundred meters through air at sea level. At 40 m, the fluence of X-rays from lightning dart leaders is roughly 1000 MeV/m^2, composed of approximately a few thousand photons per square meter, thus requiring a camera with a large effective area to detect enough photons to produce an image.

[6] The camera described in this paper is 0.64 m wide and 1.25 m long, with 1.27 cm thick lead sheets completely surrounding the camera on all sides, except for a 7.62 cm diameter circular "pinhole" aperture at the front of the camera. Figure 1 shows a photograph of the camera with the 14 m tall rocket-launch tower in the background, and Figure 2 shows a schematic diagram of the camera. Both the pinhole and the detectors are the same diameter, so there is no overlap in the field of view of neighboring detectors. The lead sheets, which together weigh more than 550 kg, are mounted on a 0.64 cm thick welded steel box (with the pinhole aperture open). This box provides the structural support, and it also provides an absorber for the fluorescent X-ray emission lines. The entire lead and steel structure is enclosed in a 0.16 cm thick aluminum outer box to exclude water, light, and RF noise. The only material covering the pinhole aperture is the 0.16 cm thick aluminum, which allows X-rays with energies as low as about 30 keV to enter unimpeded.

[7] The image plane, which is adjustable, was placed 32 cm behind the pinhole aperture, giving a field of view of about ±38° in both the vertical and horizontal directions. The elevation of the camera is adjustable between 0 and 50° from the horizontal, and the camera may be pointed in any azimuthal direction. The image plane consists of 30 7.62 cm diameter × 7.62 cm long NaI(Tl) scintillators mounted on 7.62 cm diameter photomultiplier tubes (PMTs), resulting in a spatial resolution of 4° to 8°. The PMT bases each have their own internal high-voltage (HV) supplies and HV divider chains. The signals from the PMT anodes are transmitted via 60 m long, 50 Ω double-shielded BNC cables to 2 Yokogawa DL 750 ScopeCorders that simultaneously record the 30 PMT anode channels at a sampling rate of 10^7 sample/s for a total of 2 s with 1 s of pretrigger. The data acquisition is initiated by the electrical current measurement from the lightning, which is also recorded. To reduce electrical noise, the data acquisition system is enclosed in a shielded metal trailer powered by a generator. The signal cables plus 12 V power cables are run from the trailer to the camera through a metal pipe. As a result, the camera, cables, data acquisition system, and power supplies are all effectively enclosed in a single Faraday cage.

[8] The X-ray camera was first operated at the ICLRT during the summer of 2010. For the experiments reported here, the camera was placed 44 m from the rocket-launch tower, from which lightning was triggered, and was pointed

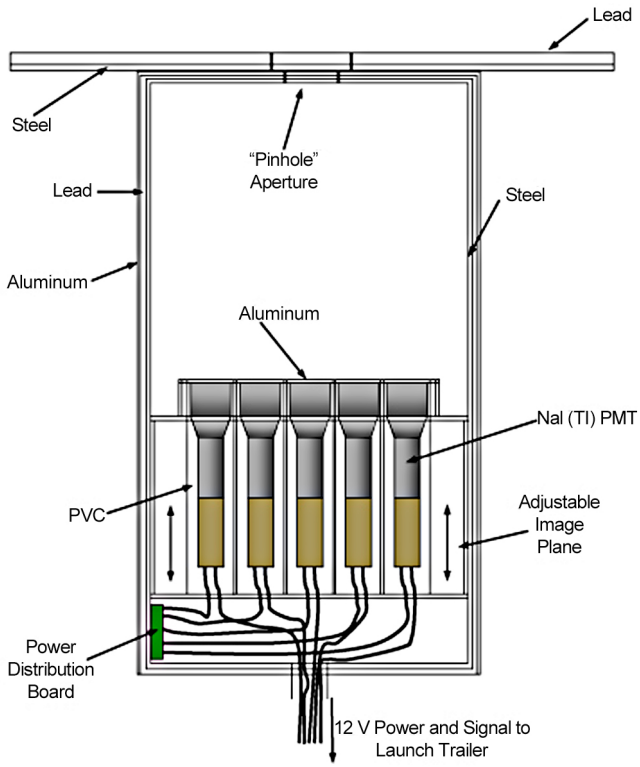

Figure 2. Schematic diagram of the X-ray lightning camera. The camera is 0.64 m wide and 1.25 m long, with 1.27 cm thick lead sheets completely surrounding the camera on all sides, except for a 7.62 cm diameter circular "pinhole" aperture at the front of the camera. The lead sheets, which together weigh 550 kg, are mounted on a 0.64 cm thick welded steel box (with the pinhole aperture open). For the observations reported here, the additional lead and steel plate seen at the top of the camera was not installed. The entire lead and steel structure is enclosed in a 0.16 cm thick aluminum outer box to exclude water, light, and RF noise (not shown). The camera uses 30 7.62 cm diameter NaI/Photomultiplier to record the X-rays passing through the pinhole aperture.

at the tower top and the lightning channel above at a 49° elevation. The wide field of view (±38° vertical and horizontal) allows emissions from slightly above the ground, including the launch tower, to near vertical to be viewed. Figure 3 shows the rocket-and-wire-triggered lightning that was produced on 15 July 2010, which resulted in the first lightning X-ray images, reported here.

3. Observations

[9] Because the lightning dart leaders and hence the X-ray source regions are moving at a significant fraction of the speed of light, the entire lightning process has a duration of only a few microseconds as observed in X-rays. As a result, it is critical to take account of propagation delays, including delays caused by the X-rays propagating from the source to the camera and delays caused by signals traveling along the BNC and fiber-optic cables. We define for each stroke the time $t = 0$ to be the time measured at the launch tower at which the return stroke current rises to half of its peak value (the risetime is in the 100 ns range). In this paper, observations are presented either in terms of the emission time, i.e., the time at which the X-rays were emitted from the source, or in terms of the observation time, i.e., the time at which the X-rays were recorded by the NaI(Tl)/PMTs inside the camera. The former was calculated from the latter by calculating the propagation time of the X-rays from the observed position along the lightning channel to the camera. As an example, X-rays take 0.15 μs to travel from the top of the launch tower to the camera.

[10] Each pixel in the camera corresponds to the output of one NaI(Tl)/PMT detector. These detectors produce a characteristic waveform that is easily distinguishable from RF noise. An X-ray that deposits its energy in the NaI crystal produces a short (negative) pulse with a very fast risetime (leading edge) and a 0.23 μs exponential falltime caused by the decay of the NaI scintillation light. Figure 4 shows 15 μs of data from a vertical line of detectors recorded for a rocket-triggered lightning stroke on 15 July 2010. The waveforms are for six NaI/PMT detectors viewing the lightning channel

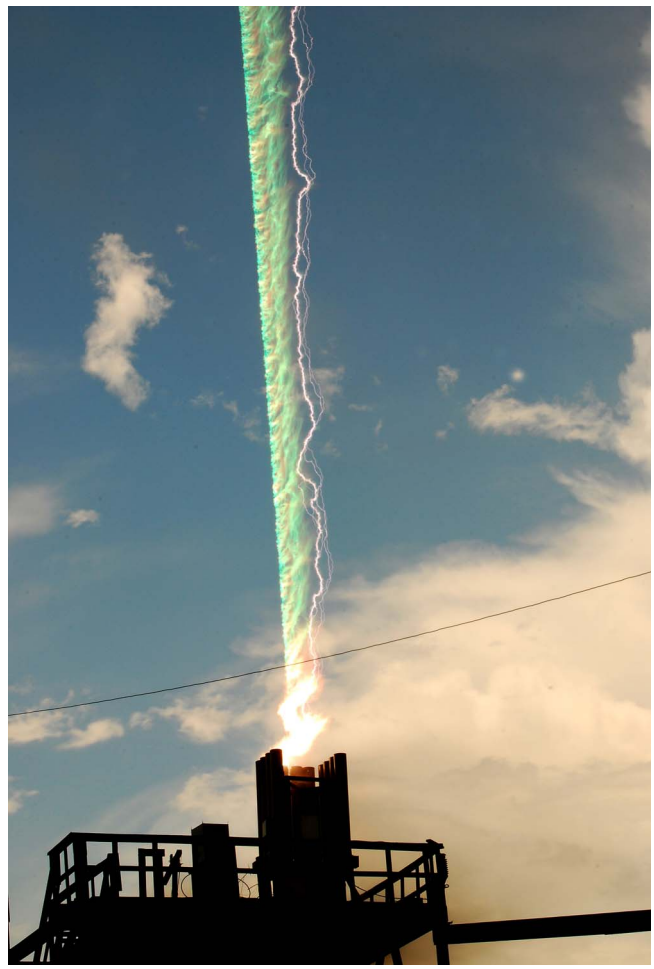

Figure 3. Photograph of the first rocket triggered lightning flash described in this report, recorded on 15 July 2010. The exploded triggering wire is on the left, the wind-separated dart leader-return stroke channel on the right. The rocket-launch tubes, also visible on top of the tower in Figure 1, can be seen at the bottom of the picture (courtesy of D. Hill).

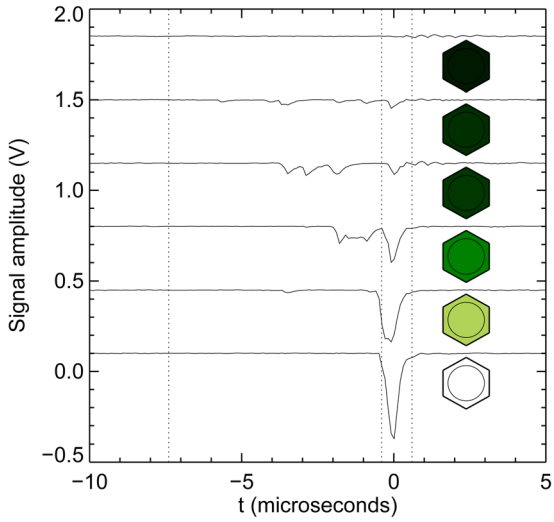

Figure 4. Raw waveforms from NaI/PMT detector anodes, arranged from (bottom) lowest to (top) highest viewing angles for the 15 July 2010 lightning. Each negative pulse corresponds to the detection of either a single X-ray or gamma ray or the detection of fast pulses of X-rays. The colored hexagons, which are used in Figures 5–8, show how the integrated pulses are converted to colors in the images. The circles show the size of the NaI detector faces relative to the size of the hexagons. The dotted lines indicate the time interval used for the two exposures in Figures 5 and 6. The return stroke occurred at time $t = 0$ in the figure.

from roughly 12 m (bottom trace) to 300 m (top trace) above the ground. The return stroke had a peak current of 22 kA and occurs (as previously noted, half of peak current on the rising front) at time $t = 0$ on the plot. For times $t < 0$, a dart leader descended downward from the thundercloud toward the ground. More specifically, this leader was a so-called "chaotic" leader, which apparently differs from typical dart leaders in producing more and more random RF and energetic radiation emissions. All the negative pulses seen before $t = 0$ in this figure correspond to the detection of X-rays from lightning. A pulse height of 0.05 V on the plot corresponds to 662 keV of energy, determined from calibration with a Cs-137 radioactive source. The natural background rate of each detector is about 40 counts/s above 100 keV, and so the probability that even one of the pulses seen in the figure is due to background is only 0.001. Because NaI/PMT detectors record only the total deposited energy, it cannot be determined from these waveforms if the pulses are due to individual gamma ray photons or multiple X-rays arriving simultaneously. Previous studies have found that the larger pulses are often multiple X-rays with energies typically in the few hundred keV range [*Dwyer et al.*, 2004; *Saleh et al.*, 2009]. In this paper, we report evidence that some of the larger detected pulses are also due to MeV gamma rays.

[11] In order to convert the waveforms from the 30 detectors into a visual image, the signal size is converted to colors, as shown in Figure 4. Since we recorded a separate image every 0.1 μs, movies of the lightning's X-ray emissions can be made. For the first image presented below (Figure 5) all data from each channel are summed between the observation times −7.4 μs and −0.4 μs, between the first two vertical dotted lines in Figure 4. The second image presented below (Figure 6) is summed between the observation times −0.4 μs and 0.6 μs, between the last two vertical dotted lines in Figure 4.

[12] The first image of lightning's X-ray emissions (Figure 5) is for a 7 μs exposure during the dart leader phase and excludes the attachment process to the tower and the return stroke, which occur after −0.4 μs. In other words, this is a view of lightning in X-rays as it travels downward through the air. The color scale ranges from no detected X-rays, in black, to the maximum deposited X-ray energy recorded, in white. Note that each detector records multiple X-rays, so the deposited X-ray energy can be much greater than the average energy of each X-ray photon, which is likely of the order of a couple hundred keV [*Dwyer et al.*, 2004; *Saleh et al.*, 2009]. To help the reader interpret the image, we have added to Figure 5 (and subsequent figures) an illustration of the rocket-launch tower (to scale). Also included is the approximate lightning channel location at the end of the exposure as estimated by a high-speed video camera. The location of the channel was found using two 3.33 μs frames from the video camera to calculate the leader speed and assuming the leader reached the top of the tower at the start of the return stroke.

[13] As can be seen in Figure 5, the downward propagating leader in the center shines the brightest in X-rays, with some X-rays detected in a diffuse glow around the channel. All nonblack hexagons in the image represent significant X-ray emissions from lightning. The diffuse glow away from the

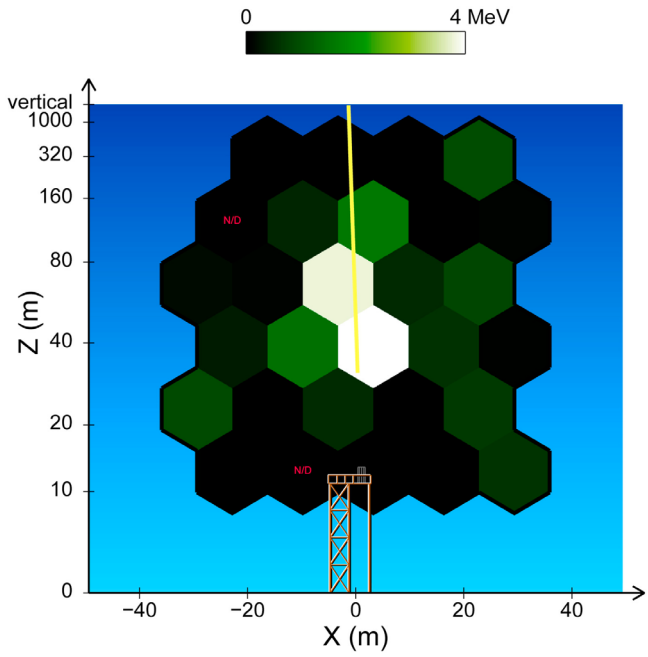

Figure 5. First image of the X-ray emission from lightning, recorded on 15 July 2010. The exposure is for observation times from −7.4 to −0.4 μs. The rocket-launch tower is illustrated at the bottom along with the approximate location of the lightning channel. The color scale ranges from no detected X-rays in black to 4 MeV of deposited X-ray energy in white.

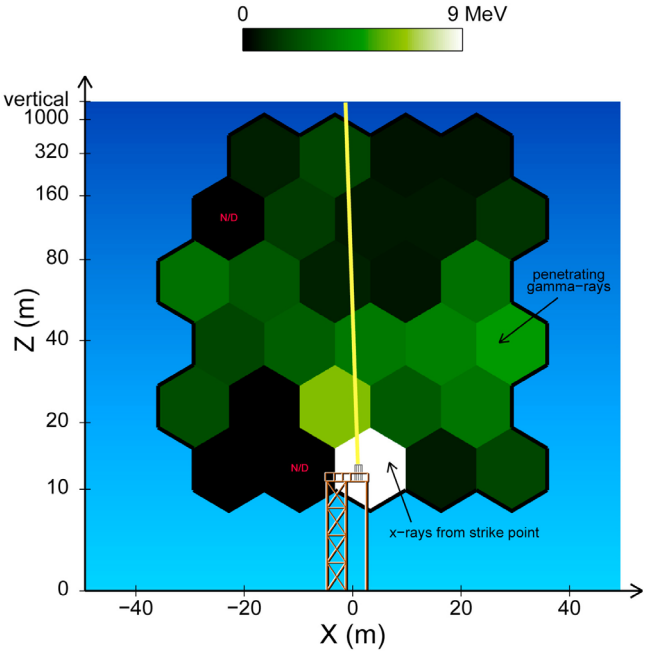

Figure 6. Image of the X-ray emission from lightning. The image is for the same stroke as that in Figure 4 but recorded for the period 1 μs after the first image. The exposure is for observation times from −0.4 to 0.6 μs. The color scale ranges from no detected X-rays in black to 9 MeV of deposited X-ray energy in white. The diffuse emission, labeled "penetrating gamma rays," originated from the tower region but passed directly through the lead and steel mask.

channel, which is a common feature of all the X-ray images produced so far, will be discussed further below.

[14] As can be seen in Figures 5, the detectors form a 30 element hexagonal array. Although the face of each detector is in fact circular, for clarity we color in the hexagons rather than just the circles (see Figure 4), interpreting the data from each detector as representing the average emission from each hexagon. We also note that two of the detectors were not operational during this flash and so are labeled N/D (no data) in the images.

[15] Figure 6 shows an image of lightning as seen in X-rays for a 1 μs exposure (−0.4 to +0.6 μs) that includes the attachment process to the tower and perhaps the start of the return stroke. Compared to Figure 5, this exposure looks significantly different. The fact that Figure 6 ends only 1 μs after the first exposure makes clear the need for high-speed measurements. The most intense emission originates from the vicinity of the launch tower, presumably associated with the attachment of the lightning to the tower (the so-called attachment process).

[16] In addition, a substantial diffuse component is visible in the surrounding detectors. This diffuse component may be due to either the X-ray emission from a diffuse source (e.g., streamers), from Compton scattering of X-rays (in the air or inside the camera) emitted from the leader front, or from some high-energy photons penetrating the lead shield. Inspection of the individual X-ray pulses shows that this component arrives simultaneously, within about 40 ns, of the bright attachment component. (Note that the pulse shapes of the NaI/PMT detectors are fit to the data to achieve a more precise timing than the digitization time.) Thus, this diffuse component could not have originated more than about 10 m from the source region of the attachment process. Because these X-ray pulses arrive within 40 ns of each other, the path lengths of the X-ray photons cannot differ by more than about 10 m, and so Compton scattering of the X-rays in air is unlikely to be the source of the diffuse component in this case. In addition, Compton scattering within the camera (e.g., between detectors) is expected to be small, which is verified by the relatively small size of the diffuse component in the previous image. The pulse shapes and deposited energy of the diffuse component in Figure 6 are consistent with X-rays in the MeV range, i.e., gamma ray energies. In other words, when the detector response function is fit to the X-ray data, it is found that the gamma ray pulses are both large, with ~MeV of deposited energy, and have pulse shapes consistent with single detected photons. On the other hand, most X-ray pulses associated with the channel emission are a clear superposition of many photons with an overall pulse width up to about 1 μs.

[17] For X-ray energies above about 400 keV, the energy deposited in all of the detectors from X-rays and gamma rays passing directly through the lead is comparable to the energy deposited in the detectors via the pinhole aperture. In other words, the lead and steel shielding material that surrounds the camera becomes transparent to X-rays and gamma rays above about 400 keV, allowing all 30 detectors to view the tower region. Since some energetic photons do not need to pass through the pinhole aperture to be detected, they appear as a diffuse emission even though they were produced in the tower region as part of the attachment component.

[18] In Figure 6, it can be seen that the diffuse component does not appear completely uniform. This can be understood from the fact that the detectors shown in the top of the image view the attachment region through the lead on the bottom of the camera, whereas the rest of the detectors view the attachment region through the lead in the front of the camera. Because the angles at which the X-rays passed through the lead sheets were different, with about twice the thickness traversed by the X-rays hitting the upper detectors in the image, fewer penetrating X-ray should be detected near the top of the image. In addition, if the diffuse component is composed of high-energy X-rays with just a few X-rays per tube being detected, fluctuations in the deposited energies are expected to be large.

[19] It is interesting that lightning emissions can be viewed easily through 1/2 inch (1.27 cm) of lead plus 1/4 inch (0.635 cm) of steel. On the other hand, because the diffuse component seen during the dart leader phase in Figure 5 is mostly composed of smaller pulses, <400 keV, penetrating gamma rays are probably not the main source of this component. Interestingly, the X-ray emission during the attachment process shown in Figure 6 was more than twice as bright as the emission during the dart leader phase shown in Figure 5. Further analysis and modeling will be required to further identify the nature of the diffuse emissions.

[20] On 13 August 2010, a rocket-triggered lightning flash was produced that had nine leader-return stroke sequences. Of these, the third stroke was by far the brightest

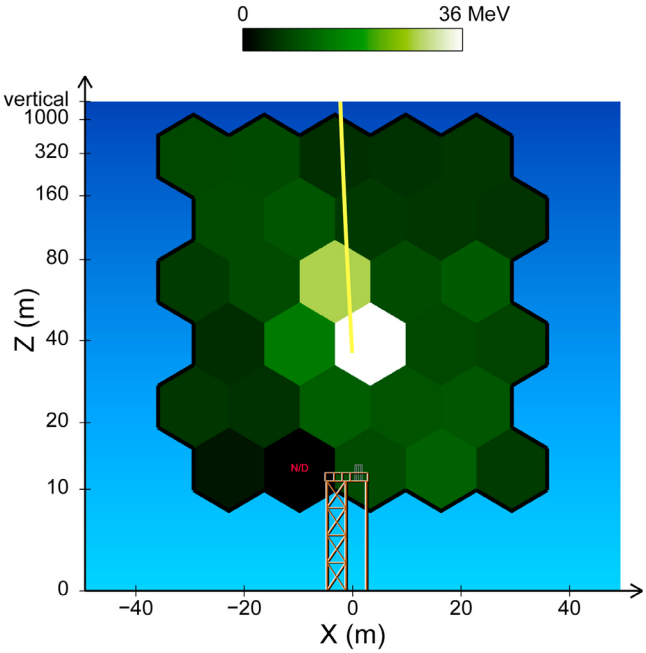

Figure 7. Image of the X-ray emission from lightning, recorded on 13 August 2010. The exposure is for observation times from −0.73 to −0.23 μs. This corresponds to the emission times from −0.96 μs to −0.41 μs. The rocket-launch tower is illustrated at the bottom along with the approximate location of the lightning channel. The color scale ranges from no detected X-rays in black to 36 MeV of deposited X-ray energy in white.

in X-rays. This stroke also had the largest peak current, 28 kA. Close electric field derivative (*dE/dt*) waveforms exhibited clear pulses during the 10 μs prior to the stroke. Like the 15 July 2010 leader, this leader was a so-called chaotic leader. These *dE/dt* pulses allowed the location of the leader front to be found as a function of time using a time-of arrival (TOA) technique [*Howard et al.*, 2008, 2010]. Figure 7 shows an X-ray image of the third stroke for a 0.5 μs exposure with observations times of −0.73 to −0.23 μs before the return stroke. This corresponds to the emission times from −0.96 to −0.41 μs. The approximate lightning channel location at end of the exposure as measured by the *dE/dt* TOA technique is also shown.

[21] This 13 August 2010 event was significantly brighter in X-rays than the event of 15 July 2010 discussed above. As a result, it is possible to make a series of images showing the progress of the lightning as it propagates to the ground. Figure 8 shows successive 0.1 μs images of the X-ray emission from the 13 August 2010 dart leader. The first image is in the upper left corner, and time progress from left to right. The exposures cover the observation times from −1.53 to +0.07 μs. This corresponds to the emission times from −1.94 to −0.087 μs. The X-ray source can clearly be seen descending with the leader *dE/dt* radiation, both at the leader front. As seen in Figures 7 and 8, there is also a considerable diffuse component. As discussed above, this diffuse component may be from a truly diffuse X-ray emission (e.g., X-ray emission from the streamer zone), from Compton scattering, or from high-energy photons penetrating the lead shield. All three of these possibilities are true X-ray emissions from the lightning and not from the background, which is negligible. In addition, all three contributions to the diffuse component may be occurring at the same time, and the relative importance of each contribution may vary with time. For example, during some time periods the energy spectrum may harden, resulting in more high-energy X-rays that penetrate through the lead. This apparently occurs during the attachment process of the 15 July 2010 leader. On the other hand, for the 13 August 2010 leader, so much energy is being deposited in the detectors that it is difficult to tell how much of the diffuse component is coming from penetrating gamma rays.

[22] In order to measure the speed of the descending leader, the diffuse component is subtracted from the channel data. The contribution of the diffuse component along the channel is estimated by first measuring the diffuse component from the 17 operating PMTs to the two sides of the channel. The vertical profile of this diffuse component is then fit to the channel data (not including the peak). This fitted diffuse component is then subtracted from the channel data, allowing the average position of the peak to be determined. This is illustrated in Figure 9, which shows the vertical profile of the X-ray source along with the diffuse component. The average position (weighted with the signal size of each detector) of the X-ray source is also plotted. This average position in the detector plane is converted to an angle, and the intersection with the lightning channel is then found to calculate the vertical height of the source. This height of the X-ray source versus emission time is plotted in Figure 10 (top) along with the height of the source as measured by the *dE/dt* pulses. The error bars are the RMS positions divided by the square root of the estimated number of detected X-rays (assuming an average X-ray energy of 200 keV). As long as the vertical distribution of the X-ray source is broader than the vertical resolution of each detector (which it is, as seen in Figure 9) then the average may be found with much better precision than the resolution of individual detectors. Figure 10 (bottom) shows the current measured at the tower. The excellent agreement between the X-ray source location and the location of the lightning leader front as measured by *dE/dt* pulses shows that the X-ray source is collocated with the front of the dart leader channel and moves downward at the same speed. The downward vertical speed of this source is 4.5×10^7 m/s, nearly 1/6 the speed of light. This speed is in the upper range of recorded dart leader speeds [*Rakov and Uman*, 2003], as is characteristic of chaotic leaders.

4. Conclusions

[23] The results presented in this paper demonstrate the viability of using X-ray imaging to study lightning, give initial results establishing the spatial and temporal connection between the dart leader and the X-ray source, and show that the lightning produces gamma rays in the MeV range. Although, in these first observations of X-rays from lightning, we make no attempt to establish general properties that apply to all lightning and are not attempting a statistical study, we have found that for the two lightning events studied in this paper the X-ray source is located near and descends with the leader front. Because the X-rays likely

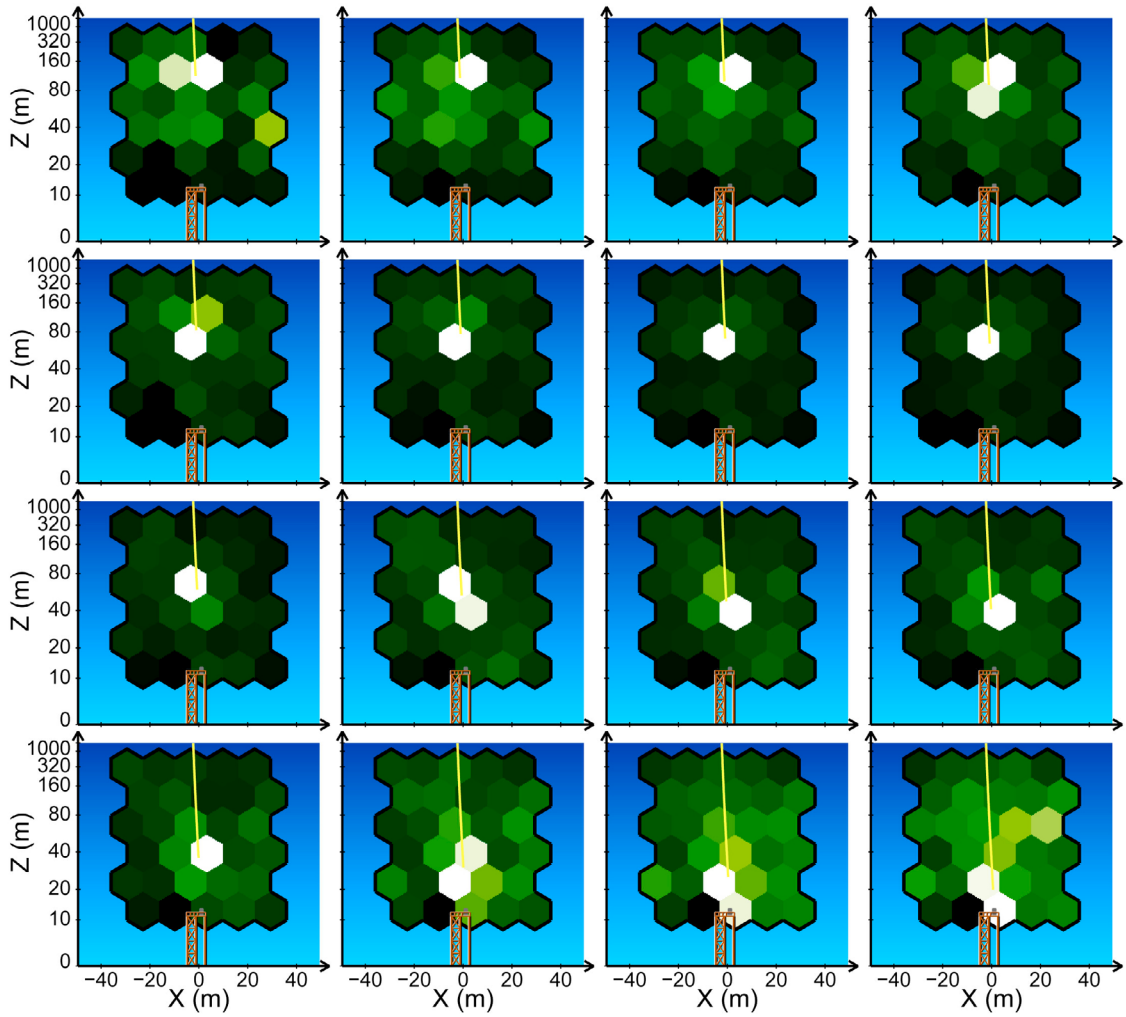

Figure 8. Successive 0.1 μs images of the X-ray emission from lightning, recorded on 13 August 2010. The first image is in the upper left corner and time progress is from left to right. The exposures cover the observation times from −1.53 to +0.07 μs. This corresponds to the emission times from −1.94 to −0.087 μs. The rocket-launch tower is illustrated at the bottom along with the approximate location of the lightning channel. The color scale for each image has been adjusted so that the detector with the maximum deposited energy appears as white. This maximum deposited energy is 5.5 MeV in the first image, increases as the lightning approaches the ground, reaching a maximum of 28.2 MeV in the eleventh image, and then decreases to 16.6 MeV in the last image.

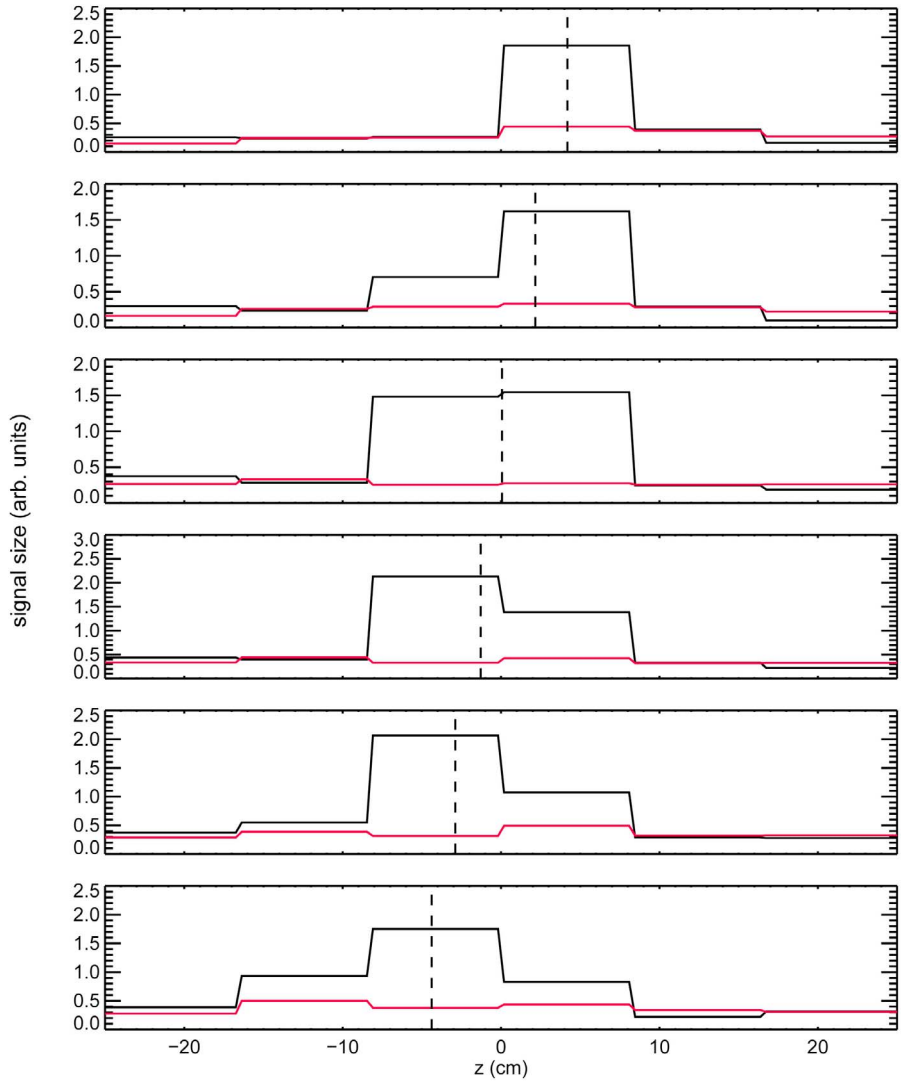

Figure 9. Histogram of X-ray signals from the NaI/PMT detectors along the vertical lightning channel. The horizontal axis is the vertical position in the detector plane, showing the six vertical rows of PMT. The exposures cover the observation times from −0.83 to −0.23 μs. This corresponds to the emission times from −1.07 to −0.41 μs. The black data show the signals for the six PMTs viewing the channel in the center of the image. The red data show the signals from the 17 operating PMTs to the two sides of the channel, fit to the black data away from the peak. The vertical dashed lines show the average position calculated after subtracting the red data (diffuse component) from the black data (channel component). These average positions are used to calculate the height of the source versus time, as plotted in Figure 10.

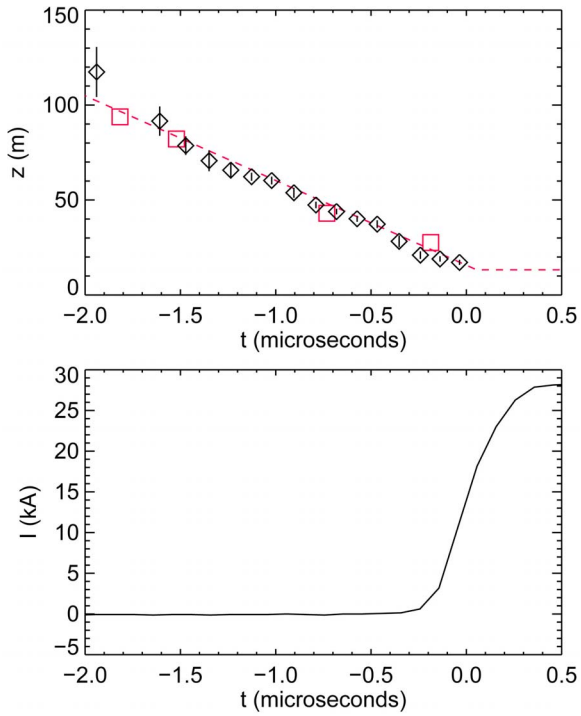

Figure 10. (top) Average vertical position of the X-ray emission versus emission time, showing that the X-ray source propagated down with the dart leader. The black diamonds are the average height of the X-ray source (see Figure 9), assuming that the source originates from the lightning channel. The red squares show the height of the lightning as measured by a TOA technique using *dE/dt* data. The straight line is a fit to the *dE/dt* data, ending at the top of the launch tower. The line corresponds to a downward dart leader velocity of 4.5×10^7 m/s. (bottom) Electrical current measured at the launch tower.

originate from runaway electrons accelerated by very strong field (>30 MV/m), these results suggest that such strong fields, which greatly exceed the conventional breakdown field, are common near the leader front. In addition, the potential differences experienced by the runaway electrons appear to reach at least 1 MV for regions where the field is greater than the runaway electron threshold of 284 kV/m [*Dwyer*, 2003].

[24] Not every triggered lightning stroke observed during the summer of 2010 generated enough X-rays to make meaningful images, but all four of the flashes (dart leaders from two given here) recorded and analyzed had one or more strokes that made enough X-rays to produce an image. For one stroke, which had a dart stepped leader, so many gamma rays were produced that the camera body was effectively transparent for the entire event. To remedy this failure in shielding, additional lead (1.27 cm thick) and steel (0.64 cm thick) sheets have been added to the front of the camera (see Figure 2). This additional attenuation should help block the higher energy X-rays in future measurements.

[25] The dart leader and X-ray observations presented provide new insights into lightning energetics and propagation phenomena and provide potential new information on related sources of X-ray and gamma rays. For example, leader X-ray emissions from near cloud tops may be related to the production of powerful terrestrial gamma ray flashes (TGFs) and terrestrial electron flashes (TEFs) observed from space [*Fishman et al.*, 1994; *Dwyer*, 2008; *Dwyer et al.*, 2008a, *Dwyer et al.*, 2010], and leader X-ray emissions are likely associated with the X-ray emissions recently discovered from long laboratory sparks [*Dwyer et al.*, 2005b, 2008b; *Rahman et al.*, 2008; *Nguyen et al.*, 2008]. Because lightning remains poorly understood, the new observational technique demonstrated in this paper is expected to provide an important tool for studying this seemingly familiar but poorly understood phenomenon.

[26] **Acknowledgments.** We would like to thank those at Florida Tech and the University of Florida who assisted in the construction, installation, and operation of the X-ray camera. In particular, we thank B. Bailey, E. Cramer, S. Arabshahi, S. Sadighi, B. Kosar, N. Liu, C. Latham, Z. Saleh, M. Stapleton, and J. T. Pilkey. We also would like to thank members of the University of Florida Lightning Research Laboratory for producing the triggered lightning. This work was supported in part by DARPA grants HR0011-08-1-0088 and HR0011-1-10-1-0061 and NSF grant ATM 0607885.

References

Dwyer, J. R. (2003), A fundamental limit on electric fields in air, *Geophys. Res. Lett.*, *30*(20), 2055, doi:10.1029/2003GL017781.

Dwyer, J. R. (2004), Implications of X-ray emission from lightning, *Geophys. Res. Lett.*, *31*, L12102, doi:10.1029/2004GL019795.

Dwyer, J. R. (2008) The source mechanisms of terrestrial gamma-ray flashes (TGFs), *J. Geophys. Res.*, *113*, D10103, doi:10.1029/2007JD009248.

Dwyer, J. R., et al. (2003), Energetic radiation produced during rocket-triggered lightning, *Science*, *299*, 694–697, doi:10.1126/science.1078940.

Dwyer, J. R., et al. (2004), Measurements of X-ray emission from rocket-triggered lightning, *Geophys. Res. Lett.*, *31*, L05118, doi:10.1029/2003GL018770.

Dwyer, J. R., et al. (2005a), X-ray bursts associated with leader steps in cloud-to-ground lightning, *Geophys. Res. Lett.*, *32*, L01803, doi:10.1029/2004GL021782.

Dwyer, J. R., H. K. Rassoul, Z. Saleh, M. A. Uman, J. Jerauld, and J. A. Plumer (2005b), X-ray bursts produced by laboratory sparks in air, *Geophys. Res. Lett.*, *32*, L20809, doi:10.1029/2005GL024027.

Dwyer, J. R., B. W. Grefenstette, and D. M. Smith (2008a), High-energy electron beams launched into space by thunderstorms, *Geophys. Res. Lett.*, *35*, L02815, doi:10.1029/2007GL032430.

Dwyer, J. R., Z. Saleh, H. K. Rassoul, D. Concha, M. Rahman, V. Cooray, J. Jerauld, M. A. Uman, and V. A. Rakov (2008b), A study of x-ray emission from laboratory sparks in air at atmospheric pressure, *J. Geophys. Res.*, *113*, D23207, doi:10.1029/2008JD010315.

Dwyer, J. R., D. M. Smith, M. A. Uman, Z. Saleh, B. Grefenstette, B. Hazelton, and H. K. Rassoul (2010), Estimation of the fluence of high-energy electron bursts produced by thunderclouds and the resulting radiation doses received in aircraft, *J. Geophys. Res.*, *115*, D09206, doi:10.1029/2009JD012039.

Eack, K. B., W. H. Beasley, W. D. Rust, T. C. Marshall, and M. Stolzenburg (1996a), Initial results from simultaneous observation of X rays and electric fields in a thunderstorm, *J. Geophys. Res.*, *101*(D23), 29,637–29,640, doi:10.1029/96JD01705.

Eack, K. B., W. H. Beasley, W. D. Rust, T. C. Marshall, and M. Stolzenburg, (1996b), X-ray pulses observed above a mesoscale convective system, *Geophys. Res. Lett.*, *23*, 2915–2918, doi:10.1029/96GL02570.

Fishman, G. J., et al. (1994), Discovery of intense gamma-ray flashes of atmospheric origin, *Science*, *264*, 1313–1316, doi:10.1126/science.264.5163.1313.

Gurevich, A. V. (1961), On the theory of runaway electrons, *Sov. Phys. JETP*, *12*(5), 904–912.

Gurevich, A. V., G. M. Milikh, and R. A. Roussel-Dupré (1992), Runaway electron mechanism of air breakdown and preconditioning during a thunderstorm, *Phys. Lett. A*, *165*, 463–468, doi:10.1016/0375-9601(92)90348-P.

Howard, J., M. A. Uman, J. R. Dwyer, D. Hill, C. Biagi, Z. Saleh, J. Jerauld, and H. K. Rassoul (2008), Co-location of lightning leader X-ray and

electric field change sources, *Geophys. Res. Lett.*, *35*, L13817, doi:10.1029/2008GL034134.

Howard, J., M. Uman, C. Biagi, D. Hill, J. Jerauld, V. A. Rakov, J. Dwyer, Z. Saleh, and H. Rassoul (2010), RF and X-ray source locations during the lightning attachment process, *J. Geophys. Res.*, *115*, D06204, doi:10.1029/2009JD012055.

McCarthy, M., and G. K. Parks (1985), Further observations of x-rays inside thunderstorms, *Geophys. Res. Lett.*, *12*, 393–396, doi:10.1029/GL012i006p00393.

Moore, C. B., K. B. Eack, G. D. Aulich, and W. Rison (2001), Energetic radiation associated with lightning stepped-leaders, *Geophys. Res. Lett.*, *28*, 2141–2144, doi:10.1029/2001GL013140.

Moss, G. D., V. P. Pasko, N. Liu, and G. Veronis (2006), Monte Carlo model for analysis of thermal runaway electrons in streamer tips in transient luminous events and streamer zones of lightning leaders, *J. Geophys. Res.*, *111*, A02307, doi:10.1029/2005JA011350.

Nguyen, C. V., A. P. J. van Deursen, and U. Ebert (2008), Multiple X-ray bursts from long discharges in air, *J. Phys. D Appl. Phys.*, *41*, 234012, doi:10.1088/0022-3727/41/23/234012.

Parks, G. K., B. H. Mauk, R. Spiger, and J. Chin (1981), X-ray enhancements detected during thunderstorm and lightning activities, *Geophys. Res. Lett.*, *8*, 1176–1179, doi:10.1029/GL008i011p01176.

Rahman, M., V. Cooray, N. A. Ahmad, J. Nyberg, V. A. Rakov, and S. Sharma (2008), X rays from 80-cm long sparks in air, *Geophys. Res. Lett.*, *35*, L06805, doi:10.1029/2007GL032678.

Rakov, V. A., and M. A. Uman (2003), *Lightning Physics and Effects*, Cambridge Univ. Press, New York.

Saleh, Z., J. Dwyer, J. Howard, M. Uman, M. Bakhtiari, D. Concha, M. Stapleton, D. Hill, C. Biagi, and H. Rassoul (2009), Properties of the X-ray emission from rocket-triggered lightning as measured by the Thunderstorm Energetic Radiation Array (TERA), *J. Geophys. Res.*, *114*, D17210, doi:10.1029/2008JD011618.

Shaw, G. E. (1967), Background cosmic count increases associated with thunderstorms, *J. Geophys. Res.*, *72*, 4623–4626, doi:10.1029/JZ072i018p04623.

Tsuchiya, H., et al. (2007), Detection of high-energy gamma rays from winter thunderstorms, *Phys. Rev. Lett.*, *99*, 165002, doi:10.1103/PhysRevLett.99.165002.

Wilson, C. T. R. (1925), The acceleration of beta-particles in strong electric fields such as those of thunder-clouds, *Proc. Cambridge Philos. Soc.*, *22*, 534–538, doi:10.1017/S0305004100003236.

J. R. Dwyer, H. K. Rassoul, and M. Schaal, Department of Physics and Space Sciences, Florida Institute of Technology, Melbourne, FL 32901, USA.

D. Hill, D. M. Jordan, and M. A. Uman, Department of Electrical and Computer Engineering, University of Florida, Gainesville, FL 32611, USA.